
Article:
Bentley, M A, Taniuchi, R, Wadsworth, R et al. (2026) Collapse of Nuclear Collectivity along the N=Z Line. Physical Review Letters. 152501. ISSN: 1079-7114

https://doi.org/10.1103/r6ns-ypw8

Collapse of Nuclear Collectivity along the $N = Z$ Line

M. A. Bentley,[1,*] R. Taniuchi,[1] R. Wadsworth,[1] H. Iwasaki,[2,3] D. D. Dao,[4] F. Nowacki,[4] M. J. Basson,[2,3] T. Beck,[2,†] B. Cederwall,[5] J. Chen,[2,3] S. Chen,[1] J. Dobaczewski,[1,6] M. Doncel,[7] A. Douglas,[2,3] P. Farris,[2,3] A. Gade,[2,3] S. A. Gillespie,[2] A. M. Hill,[2,3] D. G. Jenkins,[2,1] J. Chung-Jung,[2,3] S. M. Lenzi,[8] W. Marshall,[1] S. Paschalis,[1] J. Pereira,[2] X. Pereira-Lopez,[9] M. Petri,[1] R. Salinas,[2,3] A. Sanchez,[2,3] J. A. Swartz,[2] C. Tinson,[2,3] D. Weisshaar,[2] and K. Wimmer[10]

[1]*School of Physics, Engineering and Technology, University of York, Heslington, York, YO10 5DD, United Kingdom*
[2]*Facility for Rare Isotope Beams, Michigan State University, East Lansing, Michigan 48824, USA*
[3]*Department of Physics and Astronomy, Michigan State University, East Lansing, Michigan 48824, USA*
[4]*Université de Strasbourg, CNRS, IPHC UMR7178, 23 rue du Loess, F-67000 Strasbourg, France*
[5]*KTH Royal Institute of Technology, 10691 Stockholm, Sweden*
[6]*Institute of Theoretical Physics, Faculty of Physics, University of Warsaw, ul. Pasteura 5, PL-02-093 Warsaw, Poland*
[7]*Department of Physics, Stockholm University, 10691 Stockholm, Sweden*
[8]*Dipartimento di Fisica e Astronomia dell'Università and INFN, Sezione di Padova, I-35131 Padova, Italy*
[9]*Center for Exotic Nuclear Studies, Institute for Basic Science (IBS), Daejeon, 34126, Republic of Korea*
[10]*GSI Helmholtzzentrum für Schwerionenforschung, DE-64291 Darmstadt, Germany*

(Received 28 November 2025; revised 11 February 2026; accepted 24 March 2026; published 17 April 2026)

The lifetime of the $J^\pi = 2^+$ state in the self-conjugate ^{88}Ru nucleus has been determined in an experiment performed using rare-isotope beams provided by the new Facility for Rare Isotope Beams. This is the heaviest $N = Z$ nucleus for which such a measurement has been achieved. ^{88}Ru was populated by both one-neutron knockout and charge-exchange reactions, and the lifetime of $14.3^{+2.5}_{-3.4}$ ps was determined using the triple-foil plunger technique. The extracted electromagnetic transition strength shows that the quadrupole collectivity has dropped significantly compared with the highly deformed $N = Z$ region around $A \sim 80$. These results are compared with state-of-the-art large-scale shell-model and discrete non-orthogonal shell-model calculations. The theoretical calculations indicate a moderate triaxial deformation and suggest that low-lying states in this nucleus are no longer dominated by strong many-particle many-hole excitations, unlike the lighter, highly deformed $N = Z$ nuclei nearby.

DOI: 10.1103/r6ns-ypw8

One of the great challenges of nuclear physics is to successfully model the occurrence of nuclear collectivity, using theories rooted in the fundamental properties of the nuclear force. This challenge is especially acute in the $A \sim 80$ region for nuclei with equal numbers of protons and neutrons ($N = Z$) where, when considering states near the ground state, we find some of the most deformed and collective states in the nuclear chart (e.g., Ref. [1,2]). The high collectivity may be attributed, in part, to these nuclei lying midway between doubly magic ^{56}Ni and ^{100}Sn (strictly, $N = Z = 39$, ^{78}Y lies at the midpoint). In this naïve picture, the number of valence particle and holes can be maximized simultaneously for both types of particle, allowing for the coherent action of a large number of valence protons and neutrons. Moreover, the overlap of the proton and neutron wave functions allows for maximization of the isoscalar $T = 0$ neutron-proton interaction, known to be important in generating collectivity (see, e.g., Ref. [3]).

The reduced transition probability $B(E2)$ is the most sensitive probe of quadrupole collectivity, with the highest value of $B(E2)_{2^+ \to 0^+}$ for even-even nuclei in this region found in $N = Z$ ^{76}Sr and ^{80}Zr [1,2]. With the addition of nucleons beyond $A \sim 70$, rapidly changing nuclear collectivity is observed along the $N = Z$ line. The details of the location, and extent, of this region of extremely high collectivity presents a demanding test of our best nuclear-structure models; see, e.g., Ref. [4].

Based on algebraic symmetry arguments, the structure of these collective nuclei is predicted to involve many particle excitations across the $N = Z = 40$ shell gap. In addition, the existence of strongly quadrupole rotors also implies the presence of both pseudo-SU(3) hole orbitals and

*Contact author: michael.bentley@york.ac.uk
†Present address: KU Leuven, Instituut voor Kern- en Stralingsfysica, Celestijnenlaan 200d, 3001 Leuven, Belgium.

quasi-SU(3) particle orbitals [5]. Unfortunately, large-scale shell-model (LSSM) diagonalization becomes impossible for the most deformed $N = Z$ cases. Nevertheless, theoretical approaches based on mean-field and beyond mean-field techniques allow for modeling of such challenging cases (see, e.g., Refs. [4,6–9]). One such model, the recent variation after angular-momentum projection extension of the discrete nonorthogonal shell model, DNO-SM(VAP) [6,7], is applied in this work.

In this Letter, we present the measurement, performed at the new Facility for Rare Isoptope Beams (FRIB) [10], of the lifetime of the first excited state ($J^\pi = 2^+$) of $N = Z$ ^{88}Ru, enabling the $B(E2)_{2^+\to 0^+}$ to be determined. This is the heaviest $N = Z$ nucleus where such a measurement has been achieved. The result demonstrates a collapse in collectivity, compared with the peak around $A \sim 80$, and clearly establishes the upper boundary of the sequence of highly deformed $N = Z$ nuclei. The results are compared with LSSM and DNO-SM(VAP) [6,7,9] calculations using an extended $pf + gds$ valence space above a closed ^{56}Ni core. Additional details, beyond those described below, can be found in Supplemental Material [11].

In the experiment, a 5-kW ^{124}Xe beam, accelerated by the FRIB linear accelerator to 227 MeV/u, impinged on a 2.1 mm ^{12}C primary target within the Advanced Rare Isotope Separator (ARIS) [16], which was configured to select ^{89}Ru as the secondary beam. Three secondary beams, the $N = 45$ isotones ^{89}Ru, ^{88}Tc, and ^{85}Zr, were utilized and impinged on a 2 mm Be secondary target located in the Triple Plunger for Exotic Beams (TRIPLEX) device [17]. The target was followed by two tantalum degraders with thicknesses of 200 and 120 μm, preceded by gaps of 1.0 mm and 1.5 mm, respectively—an optimal arrangement for lifetimes in the 10–30 ps range. Incoming beam particles were identified event by event using two time-of-flight measurements: one between the ARIS focal plane and the S800 focal plane and the other between the S800 object scintillator and S800 focal plane [18]. The outgoing reaction products were identified and tracked using the S800 spectrograph, through time-of-flight, position, and energy-loss information obtained using the standard S800 focal-plane detector system; see Ref. [18] for details.

Reaction γ rays were detected by the GRETINA tracking array [19,20], comprising 12 GRETINA modules, each with four large-volume segmented HPGe crystals. Pulse-shape analysis allows for γ-ray interaction positions to be determined at a precision of a few mm [20]. The TRIPLEX device was located such that the Be target was 0.240 m upstream of the nominal GRETINA target position. The data analysis was undertaken using the GrROOT analysis package [21].

The γ-ray Doppler-shift correction was achieved by determining the velocity vector between the recoil and the first γ-ray interaction position. A reference $\beta = v/c$ was chosen, to which an event-by-event correction was applied based on the particle-tracking information. The reference β value was selected to correspond to events where the γ-ray was emitted between the two Ta degraders. With this approach, decays from states with lifetimes on the order of 10–30 ps produce three peaks, the relative intensities of which depend on the lifetime. The lowest-energy peak corresponds to decays occurring downstream of the second degrader (labeled "S" in the figures that follow), with the highest-energy peak arising from decays before the first degrader ("F"), including those within the Be target. The central peak, having the appropriate Doppler correction, is centered at the true γ-ray energy. The analysis was performed for two reaction products, ^{88}Ru and ^{84}Zr, the spectra for which are shown in Figs. 1(a) and 1(b), respectively.

Two reaction channels were used to populate ^{88}Ru: one-neutron knockout from ^{89}Ru and charge exchange from ^{88}Tc. The sum of the two channels is shown in Fig. 1(a), which shows all three components of the decay of the 616-keV $J^\pi = 2^+$ state in ^{88}Ru [22] and possibly the fast component of the 799-keV $4^+ \to 2^+$ transition. The ^{84}Zr spectrum in Fig. 1(b) was produced by one-neutron knockout from ^{85}Zr. The decay of the 539.9-keV 2_1^+ state is observed, along with decays from the 4_1^+, 6_1^+, 2_2^+, 4_2^+, and 3_1^+ states [23].

The lifetime analysis involved comparing the experimental spectra to simulations [1,24] based on the GEANT4 package [25]. The simulation accounts for lifetime effects for a given transition, including feeding from higher-lying states. The simulation models the GRETINA-detector and TRIPLEX-target geometries, as well as the beam and reaction properties, replicating the full experimental analysis approach.

In order to establish the lifetime analysis procedure for ^{88}Ru, an analysis of the 2_1^+ state in ^{84}Zr was performed using the high statistics spectrum of Fig. 1(b), allowing for crucial parameters of the simulation to be properly adjusted (see Supplemental Material [11]). In the ^{84}Zr analysis, the direct population intensities, branching ratios, and lifetimes for all the states observed, all of which have decay paths through the 2_1^+ state [23], were extracted and included in the simulation. A full analysis of these results will be presented in a future publication [26], and here we focus only on the 2_1^+ state. The simulated spectrum, including all feeding states, was fitted to the experimental spectrum along with laboratory-frame background contributions [511-keV emissions, $^{\text{nat}}$Ge(n,γ), and reactions on ^{27}Al] and a double-exponential background. The lifetime of the 2^+ state was then varied; see the inset of Fig. 1(b) for the χ^2-minimization plot, yielding 15.59(13) ps (statistical error). The red line shows the final fit. The systematic error was determined to be 1.0 ps (see Supplemental Material [11]), yielding the final result of 15.6(10) ps. The previous lifetime measurement of 20.1(11) ps [27] lies outside the error range. However, compared with the highly selective

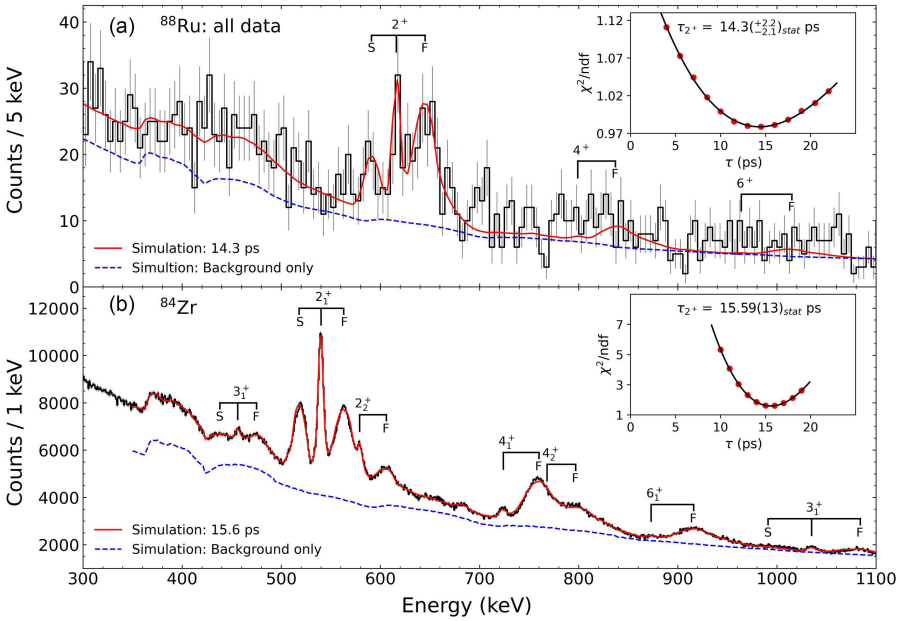

FIG. 1. (a) Spectrum of ^{88}Ru, using a reference of $\beta = 0.367$, from two reaction channels combined: one-neutron knockout from ^{89}Ru and charge exchange from ^{88}Tc. (b) ^{84}Zr from one-neutron knockout from ^{85}Zr analyzed with $\beta = 0.3535$. (a), (b): J^π label of the emitting state is placed at the true γ-ray energy. The ^{88}Ru transitions marked in (a) are 616.2 keV ($2^+ \rightarrow 0^+_{gs}$), 799.8 keV ($4^+ \rightarrow 2^+$), and 964.3 keV ($6^+ \rightarrow 4^+$). The ^{84}Zr transitions marked in (b) are 456.3 keV ($3^+_1 \rightarrow 2^+_2$), 539.9 keV ($2^+_1 \rightarrow 0^+_{gs}$), 579.3 keV ($2^+_2 \rightarrow 2^+_1$), 722.9 keV ($4^+_1 \rightarrow 2^+_1$), 787.7 keV ($4^+_2 \rightarrow 2^+_2$), 873.6 keV ($6^+_1 \rightarrow 4^+_1$), and 1035.6 keV ($3^+_1 \rightarrow 2^+_1$). The locations of the fast ("F") and slow ("S") components, if visible, are indicated. Error bars correspond to $\sqrt{N}$. Insets: χ^2 minimization analysis for the 2^+ state lifetimes. The red solid line is the final fitted simulation, and the blue dashed line is the fitted background contribution, comprising background γ-ray sources plus a double exponential.

knockout reaction used here, the measurement in Ref. [27] employed a fusion-evaporation reaction, yielding a more complex feeding pattern into the first 2^+ state. Indeed, some of the key feeding states had no measured lifetimes at the time. This may account for some of the difference in results.

The same approach was then applied to ^{88}Ru using the combined spectrum of Fig. 1(a). Simulations of the knockout and charge-exchange reactions were independently created and combined with a weighting that matches the experimental observation (~60:40 respectively). To assess the impact of feeding, a fit of the knockout spectrum was performed, yielding direct population intensities of 73%, 13%, and 14% for the 2^+, 4^+, and 6^+ states, respectively. These were included in the knockout simulation. Since the lifetimes of the 4^+ and 6^+ states cannot be determined in the current data, information from the nearby $N = 44$ isotone, ^{84}Zr, was utilized to provide a benchmark. It was assumed that the ratio $B(E2)_{4^+,6^+}/B(E2)_{2^+}$ for ^{88}Ru is the same as for ^{84}Zr measured from the high-statistics analysis presented in Fig. 1(b) [26], yielding $B(E2)_{4^+}/B(E2)_{2^+} = 1.9$ and $B(E2)_{6^+}/B(E2)_{2^+} = 0.5$. A significant error in this ratio is included as part of the systematic error; see Supplemental Material [11]. While the 2^+ is clearly present in the charge exchange reaction, there is no evidence for population of the 4^+ or 6^+ states, so only the 2^+ was included for this channel. Following the same background-fitting approach as above, the lifetime of the 2^+ state was varied, resulting in the χ^2 minimization shown in the inset of Fig. 1(a). This yields $14.3^{+2.2}_{-2.1}$ ps (statistical error). To check for consistency, the two individual reaction channels leading to ^{88}Ru were analyzed separately using the same approach as described above, and the results can be found in Supplemental Material [11].

The largest systematic uncertainty in the lifetime is associated with unobserved feeding. To benchmark this feeding, lifetime analysis was undertaken [26] of the two other $N = 44$ isotones present in the same dataset, ^{84}Zr [see Fig. 1(b)] and ^{86}Mo, both populated through one-neutron knockout. In both cases, significant feeding paths were observed to flow through the *second* 2^+ state into the first. The average impact of this feeding path on the apparent lifetime of the first 2^+ state was measured to be about +2.2 ps; see Supplemental Material [11]. The second 2^+ state in ^{88}Ru is unknown and such feeding may therefore be present but missed due to low statistics. Hence, we apply a systematic error of $^{+0}_{-2.2}$ ps to account for this possibility. The remaining systematic errors are detailed in Ref. [11]. The final result is $14.3^{+2.2}_{-2.1}(\text{stat})^{+1.2}_{-2.7}(\text{sys})$ ps. Combining in quadrature yields $14.3^{+2.5}_{-3.4}$ ps, and hence $B(E2)_{2^+\rightarrow 0^+} = 640^{+200}_{-100}$ e^2 fm^4.

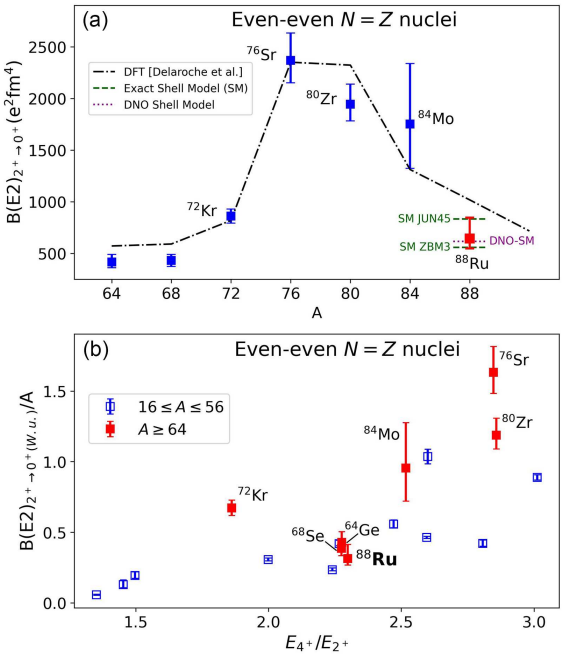

FIG. 2. (a) Experimental $B(E2)_{2^+\to 0^+}$ for even-even $N = Z$ nuclei. Dot-dashed line: the density-functional-theory results from Ref. [29]. Green dashed line: large-scale shell-model results for ^{88}Ru using two different interactions and valence spaces (see text). Purple dotted line: the DNO-SM(VAP) calculation for ^{88}Ru. (b) Experimental $B(E2)_{2^+\to 0^+}$, in Weisskopf units, per unit mass number, versus the energy ratio between the 4_1^+ and 2_1^+ states for all even-even $N = Z$ nuclei. Data are taken from Refs. [1,2,9,30–37].

Including this new result, the trend of the $B(E2)_{2^+\to 0^+}$ for even-even $N = Z$ nuclei is shown in Fig. 2(a). The result for ^{88}Ru points to a collapse in collectivity following the peak at the midshell A $\sim$ 78 and firmly establishes the upper boundary of this highly deformed region. We have also applied the approach of Casten and Zamfir [28] and examined the trend of the $B(E2)$ in Weisskopf units, normalized by mass number, as a function of (E_{4^+}/E_{2^+}); see Fig. 2(b). While originally applied to all even-even nuclei [28], only even-even $N = Z$ nuclei are shown in Fig. 2(b). The approximate correlation above $(E_{4^+}/E_{2^+}) \sim 2$ was interpreted [28] as a transition from spherical-vibrational to deformed collective rotors. The evolution from the peak of collectivity at ^{76}Sr/^{80}Zr to ^{88}Ru is clear. Notably, ^{68}Se and ^{88}Ru, which occupy the same position in the plot, both have 12 particles (holes) outside the doubly magic closures ^{56}Ni (^{100}Sn), respectively.

For an initial theoretical comparison, we use density-functional-theory calculations from Ref. [29] performed for all $Z \geq 10$ bound nuclei, from which the $B(E2)_{2^+\to 0^+}$ for $N = Z$ nuclei have been extracted [dot-dashed line in Fig. 2(a)]. These calculations employed a cranked Hartree-Fock-Bogoliubov approach mapped to a five-dimensional collective Hamiltonian, using a Gogny D1S interaction (see Ref. [29]). They were originally presented as a baseline global mapping for all nuclei based on a single approach and interaction, in order to benchmark future theoretical calculations. Despite this global approach, the calculations do a remarkable job of describing, specifically, the $N = Z$ data.

The shell model, with an appropriate valence space, is the ideal model to investigate variation of quadrupole collectivity. While LSSM calculations in the shell-model space between ^{56}Ni and ^{100}Sn, i.e., the $p_{3/2}f_{5/2}p_{1/2}g_{9/2}$ (or pfg space), are feasible (e.g., Ref. [5]), it is now well established (e.g., Refs. [4,38]) that inclusion of the $d_{5/2}$ and $s_{1/2}$ orbits is essential to properly describe collectivity for nuclei with either particle number in the mid-pfg shell. The $d_{5/2}$ and $s_{1/2}$ orbitals are the $\Delta l = \Delta j = 2$ quasi-SU(3) partners to $g_{9/2}$, and it has been proposed [5] that the quadrupole-quadrupole interaction within and between these quasi-SU(3) partner orbitals is a crucial driver of quadrupole collectivity. Moreover, the core orbitals below $N = Z = 40$ form a so-called pseudo-SU(3) space where quadrupole correlations are also known to develop favorably [4,5]. Within this $(f_{5/2}p_{3/2}p_{1/2}) + (g_{9/2}d_{5/2}s_{1/2})$ space, a new interaction, DNP-ZBM3 (referred to here as ZBM3), described first in Ref. [5], has recently been developed and applied to $N = Z$, $Z + 2$ ^{84,86}Mo [9].

With this expanded shell-model space, the new effective Hamiltonian can be diagonalized with two approaches: an exact diagonalization with the LSSM or application of the beyond-mean-field DNO shell model [6]. Although the valence-space dimensions become too large for the exact LSSM diagonalization in $N = Z$ nuclei around the peak of collectivity, they are manageable for ^{88}Ru. However, the DNO-SM calculations allow the ZBM3 effective Hamiltonian to be diagonalized efficiently in this large valence space without the same dimensional restrictions and can be applied for all $N = Z$ nuclei. A systematic study of the DNO-SM with the recent Variation After Projection (VAP) extension [7,8] applied along the $N = Z$ line is in preparation [39]. The LSSM and DNO-SM(VAP) results for ^{88}Ru, both calculated using using standard proton and neutron effective charges of $\epsilon_p = 1.5$, $\epsilon_n = 0.5$, are presented in Table I and Fig. 2(a) and are in good agreement with the data. The small difference between the two calculations, which should otherwise converge to the same value, likely arises from the degree of convergence accepted for the DNO-SM calculations and the truncation applied to the LSSM calculations (see Supplemental Material [11]).

The quasi-pseudo-SU(3) estimates (QPSU3) and Projected Hartree-Fock solutions (PHF) (see, e.g., Refs. [5,9,40]) presented in Table I provide a first glance of the contribution to the $B(E2)$ from competing many-particle many-hole structures accommodated in the present valence space. These calculations suggest only a small degree of excitation across the $N = Z = 40$ subshell closure. The same conclusion can be drawn from the

TABLE I. $B(E2;2_1^+ \to 0_1^+)$ values (in e^2 fm^4) for ^{88}Ru from quasi-pseudo-SU(3) (QPSU3), Projected Hartree-Fock (PHF), shell-model (LSSM), and DNO shell-model with variation after projection (DNO-SM(VAP)) calculations and experiment (Exp). The PHF, DNO-SM(VAP), and LSSM results use the same ZBM3 interaction and valence space. In the first column, $np-nh$ refers to the number of particle-hole excitations across the $N = Z = 40$ shell gap.

$B(E2;2_1^+ \to 0_1^+)$ (e^2 fm^4) for ^{88}Ru					
$np-nh$	QPSU3	PHF	LSSM	DNO-SM(VAP)	Exp
0p–0h	833	563	558	616	640^{+200}_{-100}
2p–2h	1185	781			
4p–4h	1600	1299			
6p–6h	2048	2147			

valence orbital occupations found in the full LSSM and DNO-SM calculations; see Supplemental Material [11]. These observations contrast with the predicted dominance of many-particle many-hole excitations around the peak of collectivity for $N = Z$ nuclei [9,39]. The DNO-SM can provide further information on the nuclear shape beyond that directly accessible in the LSSM. The expansion of the ^{88}Ru ground-state wave function in the triaxial (β,γ) plane is shown in Fig. 3 and indicates triaxial structures of only moderate deformation. This structural change at $N = Z = 44$, correlating with the reduction of collectivity compared with lighter $N = Z$ nuclei, strongly resembles the recent observation in ^{86}Mo in Ref. [9], also at $N = 44$. In both cases this likely originates from the same mechanism, i.e., the $N, Z = 50$ shell-gap opening with the $g_{9/2}$ orbital filling (e.g., Ref. [41]).

Since ^{88}Ru is now closer to the ^{100}Sn double-shell closure, one may intuitively expect that an LSSM calculation in *just* the pfg space may be sufficient. Such a calculation using the JUN45 interaction [42] using $\epsilon_p = 1.8, \epsilon_n = 0.8$ (see Supplemental Material [42]), yields

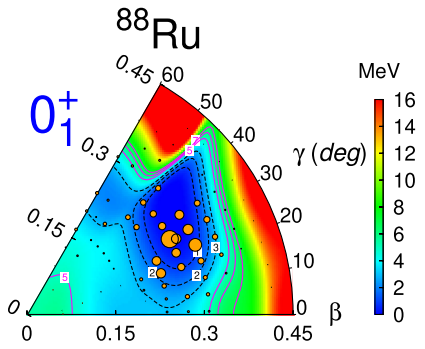

FIG. 3. Expansion of ground-state wave function in the triaxial (β,γ) plane using the DNP-ZBM3 interaction. The orange circles represent the relative contributions of given Hartree-Fock configurations.

$B(E2)_{2^+\to 0^+} = 833$ e^2 fm^4, within the experimental error range [see Fig. 2(a)]. However, the ZBM3 and JUN45 calculations yield different results in terms of wave functions and nuclear moments. The ZBM3 calculations yield a ground state dominated by 0p-0h and 2p-2h configurations with a negative spectroscopic quadrupole moment, while JUN45 produces an 4p-4h ground state with a positive value of the latter. It seems that the calculation with JUN45 overestimates the degree of particle-hole excitations to compensate for the missing quasi-SU(3) $d_{5/2}s_{1/2}$ orbitals. A previous LSSM calculation for ^{88}Ru [43] using a different interaction in the $(f_{5/2}p_{3/2}p_{1/2}) + (g_{9/2}d_{5/2})$ space [44] also produced a negative spectroscopic quadrupole moment, in contrast to the one predicted when the $d_{5/2}$ orbit is excluded. In the ZBM3 calculations the impact of the $s_{1/2}$ orbital is found to be minor in ^{88}Ru, resulting from the dominance of the 0p-0h and 2p-2h structures. However, once 6p-6h configurations are reached (see Table 1 in Supplemental Material [11]) the occupancy of the $s_{1/2}$ orbital increases significantly. These larger np-nh configurations occur as the intrinsic structure becomes more deformed, as seen, for example, in ^{84}Mo [9].

Putting these various observations together strongly suggests that the full present valence space is required for the description of the evolution of collectivity along the $N = Z$ line and of the transition toward the ^{100}Sn double-shell shell closure. Similar conclusions are drawn in the lower part of the pf shell between ^{40}Ca and ^{56}Ni where collectivity cannot be properly described using the $f_{7/2}$ orbital alone (e.g., Refs. [5,45]). The current results, and the shape predictions of the various models presented, call for future measurements, e.g., Coulomb excitation, to provide experimental information on the nuclear shape.

In conclusion, the lifetime of the $J^\pi = 2^+$ state in the $N = Z$ ^{88}Ru nucleus has been determined, the heaviest $N = Z$ system for which such a measurement has yet been achieved. The $B(E2)_{2^+\to 0^+}$ for ^{88}Ru indicates that nuclear collectivity has collapsed compared with the peak of collectivity observed around ^{76}Sr/^{80}Zr. Calculations with a new interaction developed for the $(f_{5/2}p_{3/2}p_{1/2}) + (g_{9/2}d_{5/2}s_{1/2})$ valence space have been performed. This space includes the full set of pseudo-SU(3) and quasi-SU(3) partner orbitals, predicted to be important for the description of collectivity in the nuclear shell model. Exact LSSM shell-model calculations and results from the discrete nonorthogonal shell model have been presented, both of which are shown to reproduce well the collapse in collectivity.

Acknowledgments—This work was supported by UKRI Science and Technology Facilities Council under Grants No. ST/Y000285/1, ST/V001035/1, and No. ST/P003885/1; The Royal Society; the Swedish Research Council under Grant No. 2019-0480; and the U.S. Department of Energy,

Office of Science, Office of Nuclear Physics, under Awards No. DE-SC0020451 and No. DE-SC0023633 (MSU). This material is based upon work supported by the U.S. Department of Energy, Office of Science, Office of Nuclear Physics and used resources of the Facility for Rare Isotope Beams (FRIB) Operations, which is a DOE Office of Science User Facility under Award No. DE-SC0023633. D. D. Dao and F. N. acknowledge financial support from CNRS/IN2P3, France, via ABI-CONFI Master project. D. D. D. acknowledges the financial support from CNRS/IN2P3, France, through the budget for early-career CNRS researchers.

Data availability—The processed experimental data that support the findings of this article are openly available [46].

[1] A. Lemasson, H. Iwasaki, C. Morse, D. Bazin, T. Baugher, J. S. Berryman, A. Dewald, C. Fransen, A. Gade, S. McDaniel, A. Nichols, A. Ratkiewicz, S. Stroberg, P. Voss, R. Wadsworth, D. Weisshaar, K. Wimmer, and R. Winkler, Phys. Rev. C **85**, 041303(R) (2012).
[2] R. D. O. Llewellyn *et al.*, Phys. Rev. Lett. **124**, 152501 (2020).
[3] P. Federman and S. Pittel, Phys. Rev. C **20**, 820 (1979).
[4] K. Kaneko, N. Shimizu, T. Mizusaki, and Y. Sun, Phys. Lett. B **817**, 136286 (2021).
[5] A. P. Zuker, A. Poves, F. Nowacki, and S. M. Lenzi, Phys. Rev. C **92**, 024320 (2015).
[6] D. D. Dao and F. Nowacki, Phys. Rev. C **105**, 054314 (2022).
[7] D. D. Dao and F. Nowacki, arXiv:2507.09073.
[8] D. D. Dao and F. Nowacki, arXiv:2409.08210.
[9] J. Ha, F. Recchia *et al.*, Nat. Commun. **16**, 10631 (2025).
[10] T. Glasmacher, A. Gade, G. Bollen, and J. Wei, Nucl. Phys. News **34**, 5 (2024).
[11] See Supplemental Material at http://link.aps.org/supplemental/10.1103/r6ns-ypw8 for further details of the experiment, simulation, data analysis, and theoretical models, which includes Refs. [12–15].
[12] E. Caurier and F. Nowacki, Acta Phys. Pol. B **30**, 705 (1999), https://www.actaphys.uj.edu.pl/R/30/3/705/pdf.
[13] K. W. Schmid, F. Grümmer, and A. Faessler, Phys. Rev. C **29**, 308 (1984).
[14] K. W. Schmid, F. Grümmer, and A. Faessler, Phys. Rev. C **29**, 291 (1984).
[15] K. Schmid, Prog. Part. Nucl. Phys. **52**, 565 (2004).
[16] M. Hausmann, A. Aaron, A. Amthor, M. Avilov, L. Bandura, R. Bennett, G. Bollen, T. Borden, T. Burgess, S. Chouhan, V. Graves, W. Mittig, D. Morrissey, F. Pellemoine, M. Portillo, R. Ronningen, M. Schein, B. Sherrill, and A. Zeller, Nucl. Instrum. Methods Phys. Res., Sect. B **317**, 349 (2013).
[17] H. Iwasaki, A. Dewald, T. Braunroth, C. Fransen, D. Smalley, A. Lemasson, C. Morse, K. Whitmore, and C. Loelius, Nucl. Instrum. Methods Phys. Res., Sect. A **806**, 123 (2016).
[18] D. Bazin, J. Caggiano, B. Sherrill, J. Yurkon, and A. Zeller, Nucl. Instrum. Methods Phys. Res., Sect. B **204**, 629 (2003).
[19] S. Paschalis *et al.*, Nucl. Instrum. Methods Phys. Res., Sect. A **709**, 44 (2013).
[20] D. Weisshaar *et al.*, Nucl. Instrum. Methods Phys. Res., Sect. A **847**, 187 (2017).
[21] K. Wimmer, GrROOT, https://github.com/wimmer-k/GrROOT (2012–2015).
[22] B. Cederwall *et al.*, Phys. Rev. Lett. **124**, 062501 (2020).
[23] D. Abriola, M. Bostan, S. Erturk, M. Fadil, M. Galan, S. Juutinen, T. Kibédi, F. Kondev, A. Luca, A. Negret, N. Nica, B. Pfeiffer, B. Singh, A. Sonzogni, J. Timar, J. Tuli, T. Venkova, and K. Zuber, Nucl. Data Sheets **110**, 2815 (2009).
[24] P. Adrich, D. Enderich, D. Miller, V. Moeller, R. Norris, K. Starosta, C. Vaman, P. Voss, and A. Dewald, Nucl. Instrum. Methods Phys. Res., Sect. A **598**, 454 (2009).
[25] S. Agostinelli *et al.*, Nucl. Instrum. Methods Phys. Res., Sect. A **506**, 250 (2003).
[26] M. A. Bentley *et al.* (to be published).
[27] H. G. Price, C. J. Lister, B. J. Varley, W. Gelletly, and J. W. Olness, Phys. Rev. Lett. **51**, 1842 (1983).
[28] R. F. Casten and N. V. Zamfir, Phys. Rev. Lett. **70**, 402 (1993).
[29] J. P. Delaroche, M. Girod, J. Libert, H. Goutte, S. Hilaire, S. Péru, N. Pillet, and G. F. Bertsch, Phys. Rev. C **81**, 014303 (2010).
[30] K. Starosta *et al.*, Phys. Rev. Lett. **99**, 042503 (2007).
[31] A. Obertelli, T. Baugher, D. Bazin, J. P. Delaroche, F. Flavigny, A. Gade, M. Girod, T. Glasmacher, A. Goergen, G. F. Grinyer, W. Korten, J. Ljungvall, S. McDaniel, A. Ratkiewicz, B. Sulignano, and D. Weisshaar, Phys. Rev. C **80**, 031304(R) (2009).
[32] A. Nichols *et al.*, Phys. Lett. B **733**, 52 (2014).
[33] H. Iwasaki *et al.*, Phys. Rev. Lett. **112**, 142502 (2014).
[34] K. Wimmer *et al.*, Eur. Phys. J. A **56**, 159 (2020).
[35] B. Pritychenko, M. Birch, B. Singh, and M. Horoi, At. Data Nucl. Data Tables **107**, 1 (2016).
[36] K. Arnswald *et al.*, Phys. Lett. B **772**, 599 (2017).
[37] P. Voss *et al.*, Phys. Rev. C **96**, 024305 (2017).
[38] S. M. Lenzi, F. Nowacki, A. Poves, and K. Sieja, Phys. Rev. C **82**, 054301 (2010).
[39] D. D. Dao, F. Nowacki, and A. Poves (to be published).
[40] C. W. Johnson and C. Jiao, J. Phys. G **46**, 015101 (2018).
[41] K. Sieja and F. Nowacki, Phys. Rev. C **85**, 051301(R) (2012).
[42] M. Honma, T. Otsuka, T. Mizusaki, and M. Hjorth-Jensen, Phys. Rev. C **80**, 064323 (2009).
[43] K. Kaneko, Y. Sun, and G. de Angelis, Nucl. Phys. **A957**, 144 (2017).
[44] K. Kaneko, T. Mizusaki, Y. Sun, and S. Tazaki, Phys. Rev. C **89**, 011302(R) (2014).
[45] E. Caurier, G. Martínez-Pinedo, F. Nowacki, A. Poves, and A. P. Zuker, Rev. Mod. Phys. **77**, 427 (2005).
[46] M. A. Bentley, University of York Research Database: 10.15124/f57f886f-3b85-46a5-845f-e31a007acfcd (2025).